NANO LETTERS

Letter

pubs.acs.org/NanoLett

# Enhancement of Light Absorption in Silicon Nanowire Photovoltaic Devices with Dielectric and Metallic Grating Structures

Jin-Sung Park,[†] Kyoung-Ho Kim,[†,§] Min-Soo Hwang,[†] Xing Zhang,[§] Jung Min Lee,[†] Jungkil Kim,[†] Kyung-Deok Song,[†] You-Shin No,[∥] Kwang-Yong Jeong,[⊥] James F. Cahoon,[§] Sun-Kyung Kim,*[,‡] and Hong-Gyu Park*[,†,#]

[†]Department of Physics, Korea University, Seoul 02841, Republic of Korea

[§]Department of Chemistry, University of North Carolina at Chapel Hill, Chapel Hill, North Carolina 27599, United States

[∥]Department of Physics, Konkuk University, Seoul 05029, Republic of Korea

[⊥]Department of Nano Science and Technology, Gachon University, Gyeonggi-do 13120, Republic of Korea

[‡]Department of Applied Physics, Kyung Hee University, Gyeonggi-do 17104, Republic of Korea

[#]KU-KIST Graduate School of Converging Science and Technology, Korea University, Seoul 02841, Republic of Korea

*S* *Supporting Information*

**ABSTRACT:** We report the enhancement of light absorption in Si nanowire photovoltaic devices with one-dimensional dielectric or metallic gratings that are fabricated by a damage-free, precisely aligning, polymer-assisted transfer method. Incorporation of a $Si_3N_4$ grating with a Si nanowire effectively enhances the photocurrents for transverse-electric polarized light. The wavelength at which a maximum photocurrent is generated is readily tuned by adjusting the grating pitch. Moreover, the electrical properties of the nanowire devices are preserved before and after transferring the $Si_3N_4$ gratings onto Si nanowires, ensuring that the quality of pristine nanowires is not degraded during the transfer. Furthermore, we demonstrate Si nanowire photovoltaic devices with Ag gratings using the same transfer method. Measurements on the fabricated devices reveal approximately 27.1% enhancement in light absorption compared to that of the same devices without the Ag gratings without any degradation of electrical properties. We believe that our polymer-assisted transfer method is not limited to the fabrication of grating-incorporated nanowire photovoltaic devices but can also be generically applied for the implementation of complex nanoscale structures toward the development of multifunctional optoelectronic devices.

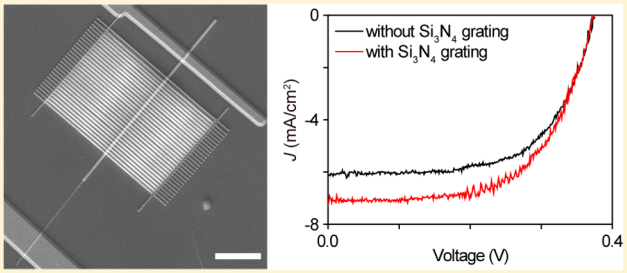


**KEYWORDS:** *Core/shell Si nanowires, photovoltaic devices, gratings, polymer-assisted transfer*



Nanowires (NWs) represent multifunctional nanoscale materials that are distinguishable from their counterpart bulk structures by prospective optical and electrical properties.[1−10] In particular, a high-refractive-index NW structure presents absorption and scattering cross sections larger than its physical cross-section,[7−12] which stimulates a motive for the development of nanoscale photodetectors,[13−17] lasers,[18−20] light-emitting diodes,[21−25] and photovoltaic (PV) devices.[9−12,26−28] More importantly, optical resonances in a NW cavity are readily tuned by adjusting their morphology and composition, via precisely programmed synthetic protocols.[7,8,10−12,28] For example, a subtle variation in the size of Si and Ge NWs has led to fine-tuning of their absorption modes.[7,8,10] A NW with a controlled cross-sectional shape can also produce high-amplitude absorption modes at specific wavelengths.[11,28] Addition of a conformal dielectric coating on Si NW PV devices leads to an approximate doubling of their absorption, as a result of amplified optical antenna effects over broadband wavelengths.[12]

Although such in situ and ex situ efforts have led to successful modulation of the optical resonances in a NW, attaining large absorption efficiency at the deep-red to near-infrared wavelengths remains a nontrivial issue, particularly for crystalline Si NW PV devices.[10−12,28] Recently, periodic-shell NWs have been synthesized with their diameter modulated along the axis, with a well-defined pitch.[29,30] Numerical simulations have showed that periodic-shell Si NWs yield significantly enhanced absorption efficiency at specific long wavelengths because they can convert the normally incident plane waves into axially propagating waveguide modes, thereby enhancing the absorption.[29,31] This suggests that increasing the morphological complexity of NWs could enable amplification of the optical resonances at specific wavelengths. Analogous to this in situ synthetic control, fabricating complex nanoscale structures and

**Received:** September 11, 2017
**Revised:** November 2, 2017
**Published:** November 17, 2017

  

DOI: 10.1021/acs.nanolett.7b03891
*Nano Lett.* 2017, 17, 7731−7736

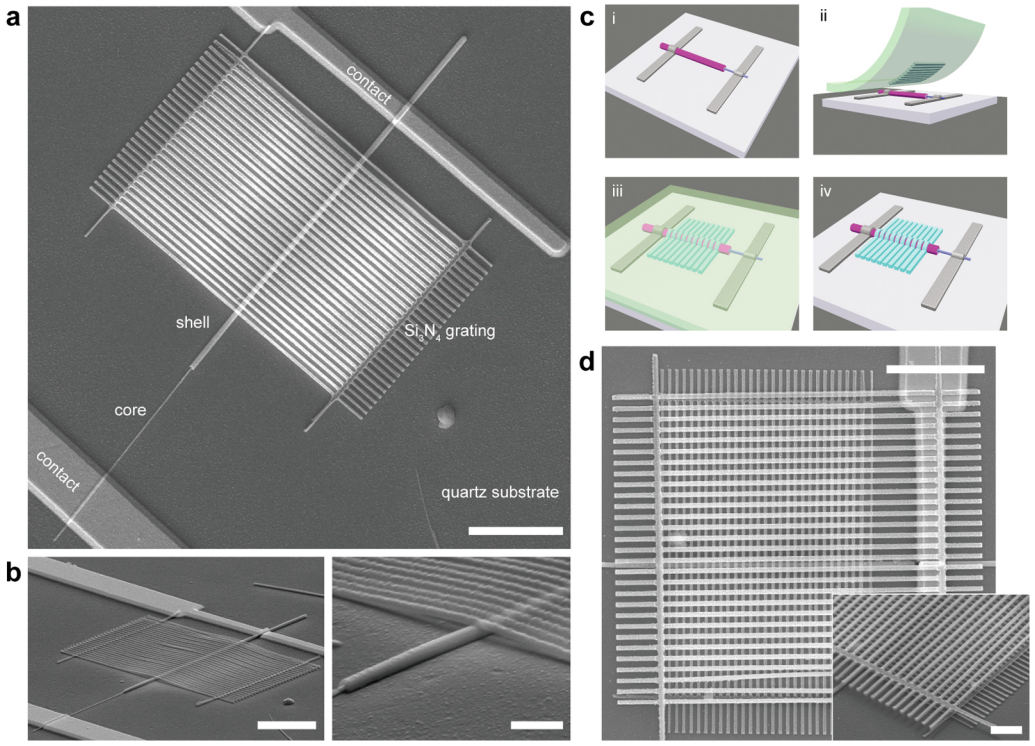


**Figure 1.** Core/shell p/in Si NW PV devices with a dielectric grating. (a) Top-view SEM image of a Si NW PV device with a $Si_3N_4$ grating. The grating partially covers the n-type shell region of the 290 nm diameter Si NW. The pitch, width, and thickness of the $Si_3N_4$ grating are 380, 190, and 140 nm, respectively. Scale bar, 5 $\mu$m. (b) Tilted-view SEM images of the device in (a). The right panel shows a magnified SEM image corresponding to the left panel. The scale bars are 5 (left) and 1 $\mu$m (right). (c) Schematic illustration of the fabrication of a Si NW PV device with a grating: (i) a NW PV device is fabricated, (ii) and (iii) well-aligned dielectric or metallic gratings attached to a PMMA layer are transferred onto the NW, and (iv) the PMMA layer is removed. (d) SEM image of a Si NW PV device with cross-stacked $Si_3N_4$ gratings. Another layer of $Si_3N_4$ grating is transferred onto the structure of (a), parallel to the NW axis. The pitch of the second grating is 570 nm. Scale bar, 5 $\mu$m. Inset, tilted-view SEM image of the cross-stacked double layers of the $Si_3N_4$ grating. Scale bar, 2 $\mu$m.

transferring them onto a NW can give rise to similar optical effects, providing a viable strategy for the development of high-efficiency NW PV devices. Here, we report Si NWs with dielectric or metallic gratings that could serve as a facile and effective approach for posthoc optical modulation. We developed a damage-free transfer method that enables the integration of NWs with complex architectures. Core/shell p/in Si NW PV devices were fabricated on a transparent quartz substrate, and light was illuminated through the quartz substrate. The absorption efficiencies of the devices with and without gratings were quantitatively assessed by directly measuring the photocurrent. Current density–voltage ($J$–$V$) transport characteristics of the NW devices were also recorded before and after the incorporation of the gratings into the same devices.

Core/shell p/in Si NWs were synthesized by the vapor–liquid–solid growth of a p-type core and the following vapor–solid growth of intrinsic and n-type shells in a chemical vapor deposition (CVD) reactor.[10,28] A 40 nm thick $SiO_2$ outer shell was uniformly coated on the grown core/shell Si NWs by plasma-enhanced chemical vapor deposition (PECVD), and the NWs were dispersed on a 200 nm thick $Si_3N_4$-coated quartz substrate. To fabricate the PV devices, n-type and intrinsic shells were partially wet-etched to expose the p-type core. Subsequently, anode and cathode electrodes were defined on the p-type core and n-type shell regions, respectively (see Methods). These NW PV devices were then integrated with $Si_3N_4$ gratings, as shown in the scanning electron microscopy (SEM) image (Figure 1a). Note that the $Si_3N_4$ grating is transferred onto the NW by a poly(methyl methacrylate) (PMMA)-assisted method[32] without any noticeable breakage or disconnected features, as is evident from the plan-view SEM images (Figure 1b). Figure 1c schematically illustrates the key processes of our transfer method. First, a grating fabricated on a donor substrate is coated with a PMMA layer and subsequently peeled off from the substrate by a selective wet-etching process. Next, the entire PMMA layer containing the fabricated grating is transferred onto a working NW device, while precisely adjusting the relative position and angle between the NW device and grating (Supporting Information Figure S1a). Eventually, the transfer process is completed by removing the PMMA layer. Three-dimensional complex nanoscale architectures can also be readily constructed by simply iterating the same transfer process. As a proof-of-concept, we fabricated two pairs of vertically cross-stacked $Si_3N_4$ gratings on top of a Si NW device with the orientations of the two grating layers perpendicular to each other (Figure 1d).

The described transfer method presents several advantages. First, it facilitates a high alignment precision of the grating in both position (a range of misalignment in position <1 $\mu$m) and orientation (a range of misalignment in angle <~3° with respect to the axis of the underlying NW), as is apparent from the SEM images (Figure 1a and Supporting Information Figure S1b–d). Second, the PMMA-assisted transfer method reduces the number of fabrication steps and successfully prevents any undesirable damage to the devices. For example, we can omit



DOI: 10.1021/acs.nanolett.7b03891
Nano Lett. 2017, 17, 7731–7736

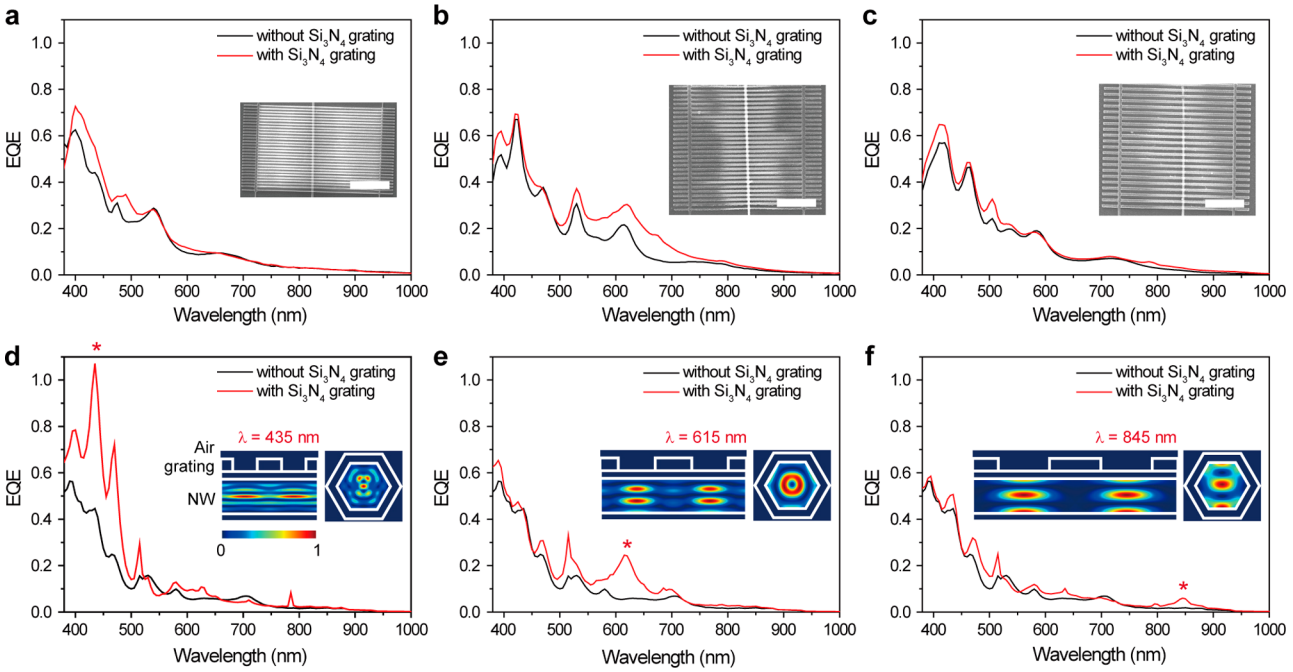


**Figure 2.** (a–c) Measured TE-polarized EQE spectra of a Si NW PV device without (black) and with (red) the $Si_3N_4$ grating. The grating pitches and widths of the grating grooves are 380 and 190 nm (a), 570 and 320 nm (b), and 800 and 380 nm (c), respectively. Insets, SEM images of the $Si_3N_4$ gratings on Si NW PV devices. All scale bars, 5 $\mu$m. The NW diameters are 290 (a), 340 (b), and 300 nm (c). In each panel, the measurements were performed using the same NW PV device, before and after transferring the grating. (d–f) Calculated TE-polarized EQE spectra of a Si NW PV device without (black) and with (red) the $Si_3N_4$ grating. For all cases, the NW diameter was set to 330 nm. The grating pitches are 380 (d), 570 (e), and 800 nm (f). The width of an individual $Si_3N_4$ grating groove is half of the given pitch. Insets, normalized absorption profiles calculated at 435 (d), 615 (e), and 845 nm (f). These wavelengths are denoted by *. Both axis-cut (left) and cross-sectional (right) absorption profiles are shown.

multiple lift-off processes for the fabrication of complex three-dimensional architectures, which could often cause breakage or disconnections in the nanostructures. In fact, a Si NW device with cross-stacked $Si_3N_4$ gratings (Figure 1d), fabricated as a proof-of-concept, could lead to significant enhancement of the light absorption by the NW. To explore this feature quantitatively, we carried out finite-difference time-domain (FDTD) simulations (Supporting Information Figure S2). The simulated absorption spectra for a Si NW device with cross-stacked $Si_3N_4$ gratings predict enhanced light absorption over a broad range of wavelengths, compared to that of a NW device without the grating or a NW device with single-stacked grating. Therefore, we believe that the described method can be used for facile integration of semiconductor NWs and various nanostructures, to achieve unique optical properties.

Next, we performed optical characterization of the NW PV devices by measuring photocurrents. The effect of one-dimensional $Si_3N_4$ grating on light absorption was examined by comparing the performance of the same NW device before and after the introduction of the grating. We measured the polarization-resolved photocurrents of the Si NW PV devices with and without the $Si_3N_4$ gratings at wavelengths ranging from 380 to 1000 nm (Figure 2a–c). The transverse-electric (TE; the electric field perpendicular to the NW axis) and transverse-magnetic (TM; the electric field parallel to the NW axis) polarized light was illuminated on the NW PV devices through the transparent quartz substrate (see Methods). To define the external quantum efficiency (EQE), the projected area of a NW was used as its physical cross-section.[10,12,28] After the EQE measurement on the NW devices without grating, $Si_3N_4$ gratings with different pitches (380, 570, and 800 nm) were transferred onto them (Figure 2a–c, insets). Here, the width of the individual $Si_3N_4$ grating groove was set to almost half of the given pitch. The measured EQE spectra reveal key absorption features of the NW PV devices related to the $Si_3N_4$ grating (Figure 2a–c and Supporting Information Figure S3a–c). First, in the devices without the grating the EQE spectra for both TE- and TM-polarized light show several absorption peaks that correspond to distinct optical resonances within the NW cavities.[10,12,28] Second, all the NW PV devices with the gratings yield a noticeable enhancement in EQE only for TE-polarized light, whereas the EQE spectra remain almost unchanged for TM-polarized light. Third, for NW PV devices with the gratings the EQE enhancement for TE-polarized light appears in different wavelength regions depending on the grating pitches; as the grating pitch increases, the wavelength of the maximum EQE enhancement tends to increase.

Since these EQE spectra were measured on the same NW PV device before and after transferring the grating onto the NW, the observed spectral changes are attributed solely to the effect induced by the $Si_3N_4$ grating. It is well-known that grating structures are useful for changing the propagation direction of light by diffraction.[33,34] When the normal incident light is illuminated on the NW through the quartz substrate, the grating can produce a wavevector component propagating along the in-plane direction of the NW axis. Indeed, the first- or second-order diffracted light appears due to the grating, which strongly depends on the wavelength and polarization of the incident light and the grating pitch (Supporting Information Figure S4a–c). Only TE-polarized light is significantly diffracted, and the wavelength of the maximum diffraction increases with increasing grating pitch. Consequently, the absorption of the TE-polarized light can be enhanced in the Si NW with grating mainly due to the first-order diffracted light in



DOI: 10.1021/acs.nanolett.7b03891
Nano Lett. 2017, 17, 7731–7736

addition to the light directly coming through the substrate, compared with that of the Si NW without the grating that absorbs light only coming through the substrate. In contrast, no enhancement is observed in the NW with the grating for the TM polarization at all the considered wavelengths, owing to weak diffraction from the grating (Supporting Information Figure S4d–f). Such polarization-dependent EQE enhancement is confirmed by numerical simulations. We calculated the absorption spectra of the Si NWs with and without the $Si_3N_4$ gratings using a finite-element method (FEM) (Figure 2d–f and Supporting Information Figure S3d–f). The calculated EQE spectra are in good agreement with the corresponding measurement results. In particular, we show the normalized absorption mode profiles at wavelengths corresponding to the enhanced EQE peaks (denoted by * in Figure 2d–f). The optical resonances with a periodic intensity variation along the NW axis are clearly observed only in the NW with the grating.

To elucidate the EQE enhancement as a function of the grating pitch, we normalized the TE-polarized photocurrents measured from the three grating-incorporated NW devices with respect to those from their bare NW device counterparts (Figure 3a). Several unique features were clearly observed. First, the wavelength of the maximum EQE enhancement for each device shows a redshift as the grating pitch of the device increases. For example, the wavelength regions of the maximal EQE enhancement are achieved in the 400–600, 600–800, and 800–1000 nm range for the NW PV devices with grating pitches of 380, 570, and 800 nm, respectively, as a result of light diffraction by gratings. In addition, the TE-polarized EQE enhancement tends to be stronger at longer wavelengths, primarily due to the lower absorption coefficient of Si.[10−12,28] This pitch-dependent EQE enhancement was reproduced well in the FEM simulation (Figure 3a, inset). Considered together, the grating is effective in increasing the photocurrent in a NW PV device at a desired wavelength of the TE-polarized incident light.

To evaluate the electrical properties of the NW PV device before and after transferring the $Si_3N_4$ grating, we measured the $J-V$ transport characteristics under 1-sun AM 1.5G illumination for the same device with and without the $Si_3N_4$ grating (Figure 3b and Supporting Information Figure S5). All the NW PV devices with gratings show that the short-circuit current density ($J_{SC}$) is enhanced but the open-circuit voltage ($V_{OC}$) is preserved or even slightly increased, compared to their bare NW devices. For example, the $J-V$ characteristics measured for the NW PV device with a grating pitch of 380 nm shows an enhancement of $J_{SC}$ of ~19.5%, but a $V_{OC}$ of 0.37 V is preserved after the grating is introduced (Figure 3b). These undeteriorated electrical characteristics support that our PMMA-assisted transfer method minimizes physical damage on the Si NW and preserves the electrical quality of the Si NW device. For comparison, we prepared a Si NW PV device with a PMMA grating that was directly fabricated on the Si NW by conventional electron-beam lithography (Supporting Information Figure S6a). In contrast to the NW devices fabricated by the transfer method, the $J-V$ transport characteristics of the NW device reveal a discernible reduction in $V_{OC}$ after the introduction of the large-area PMMA grating (Supporting Information Figure S6b). Therefore, we conclude that our transfer method is highly useful for increasing the structural complexity of Si NW devices while preserving the electrical properties and performance of the devices.

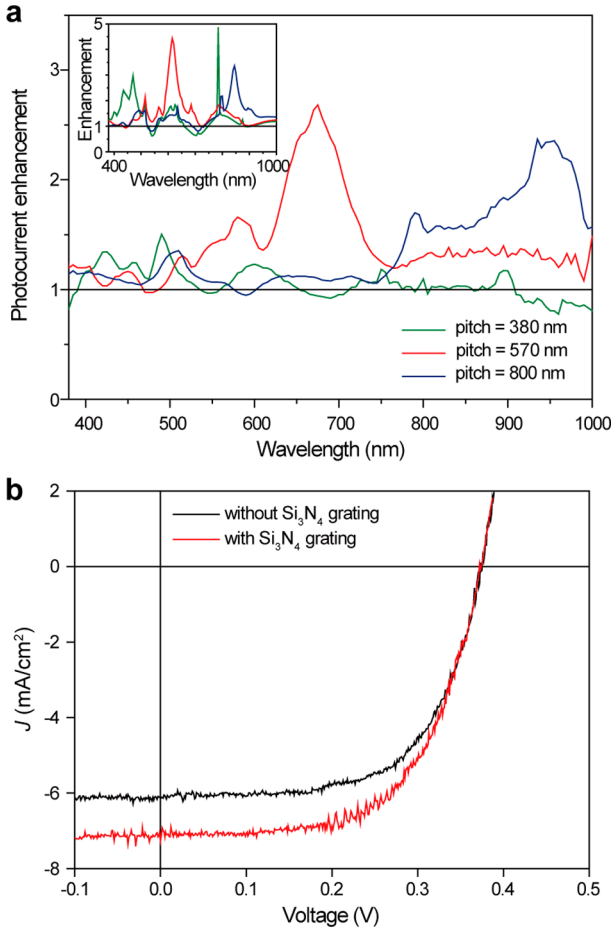


**Figure 3.** (a) Measured photocurrent enhancement as a function of the wavelength for grating pitches of 380 (green), 570 (red), and 800 nm (blue). The photocurrent enhancement is defined as the ratio of the EQE value of a NW device with a grating to that of a bare NW device. Data were taken from Figure 2a–c. Inset, calculated photocurrent enhancement as a function of the wavelength for grating pitches of 380 (green), 570 (red), and 800 nm (blue), compared with their bare NW device counterparts. Data were taken from Figure 2d–f. (b) Measured current density $J$ versus voltage characteristics under 1-sun AM 1.5G illumination, for a Si NW PV device without (black) and with (red) the $Si_3N_4$ grating. The NW diameter is 290 nm and the grating pitch is 380 nm. The short-circuit current densities $J_{SC}$ are 6.09 and 7.28 mA/cm$^2$ for the NW PV device without and with the grating, respectively. The open-circuit voltages $V_{OC}$ are 0.37 V in both cases.

Furthermore, the PMMA-assisted transfer method can be utilized to incorporate other material architectures with the NWs. In Figure 4a, we show the transfer of an Ag grating onto a Si NW PV device. The Ag grating is aligned precisely with respect to the axis of the underlying NW, similarly to the previous $Si_3N_4$ grating. We measured the $J-V$ transport characteristics for the same device before and after the introduction of an Ag grating with a pitch of 620 nm (Figure 4b). $V_{OC}$ of 0.35 V remains the same even after the integration of the Ag grating, while the $J_{SC}$ increases from 7.49 to 9.52 mA/cm$^2$. An intensified grating effect of the metal leads to ~27.1% enhancement in $J_{SC}$, which surpasses those of the previous $Si_3N_4$ grating devices. The polarization-resolved EQE spectra were also obtained for the same device with and without an Ag grating. The EQE corresponding to TE-polarized light is significantly enhanced over a wide spectral range by the Ag grating (Figure 4c), whereas the EQE corresponding to the



DOI: 10.1021/acs.nanolett.7b03891
Nano Lett. 2017, 17, 7731−7736

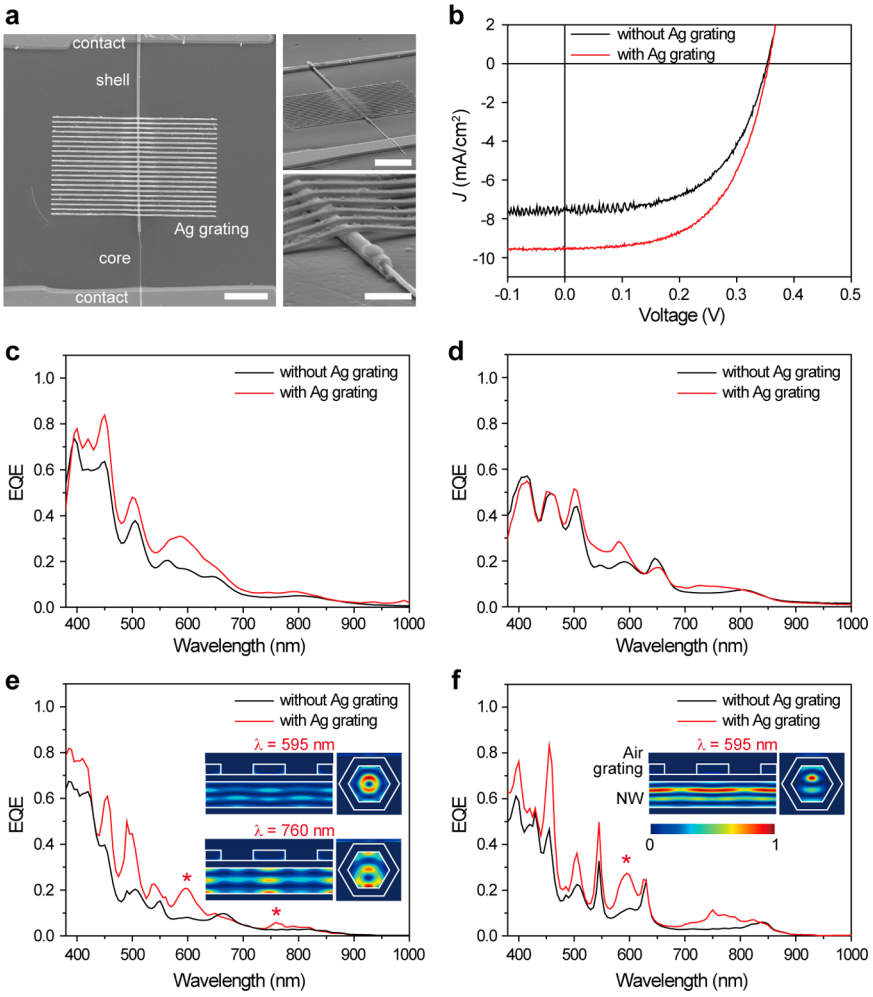


**Figure 4.** A Si NW PV device with an Ag grating. (a) Top-view (left) and tilted-view (right) SEM images of the device with the Ag grating. The diameter of the Si NW is 330 nm. The pitch, width, and thickness of the Ag grating are 620, 290, and 100 nm, respectively. The right bottom panel shows a magnified SEM image of the right top panel. The scale bars are 5 (left and right top panels) and 1 $\mu$m (right bottom panel). (b) Measured current density $J$ versus voltage characteristics under 1-sun AM 1.5G illumination, for Si NW PV devices before (black) and after (red) the transfer of the Ag grating. The NW diameter is 330 nm and the pitch of the Ag grating is 620 nm. The short-circuit current densities $J_{SC}$ are 7.49 and 9.52 mA/cm$^2$ for the NW PV device without and with the grating, respectively. The open-circuit voltages $V_{OC}$ are 0.35 V in both cases. Light was illuminated through the transparent quartz substrate. (c,d) Measured polarization-resolved EQE spectra corresponding to TE-polarized light (c) and TM-polarized light (d), for the Si NW PV devices before (black) and after (red) the transfer of the Ag grating. The NW PV device shown in panel b was used in these measurements. (e,f) Calculated TE-polarized (e) and TM-polarized (f) EQE spectra for a Si NW PV device without (black) and with (red) the Ag grating. The pitch, width, and thickness of the Ag grating are 620, 310, and 100 nm, respectively. Insets, normalized absorption profiles calculated at 595 and 760 (e), and 595 nm (f). These wavelengths are denoted by *. Both axis-cut (left) and cross-sectional (right) absorption profiles are shown.

TM-polarized light is weakly enhanced (Figure 4d). The significant EQE enhancement with respect to the TE-polarized light originates from the light diffraction along the NW axis owing to the metallic grating, which is similar to that of the dielectric grating. In case of TM-polarized light, in contrast to the dielectric grating, the reflection from the Ag grating is not negligible and an increased light absorption is observed.[35] The EQE spectra obtained by FEM simulations reproduced well the measured polarization-dependent spectra (Figure 4e,f). To better understand such EQE enhancements, we show the calculated absorption mode profiles at 595 and 760 nm (Figure 4e, inset) for the TE polarization, and 595 nm (Figure 4f, inset) for the TM polarization. These well-confined absorption intensity distributions within the NW for both TE and TM polarizations explain the observed absorption enhancements in a NW PV device with the Ag grating.

In summary, we developed a damage-free, precisely aligning, polymer-assisted transfer method that enabled the integration of Si NWs with dielectric or metallic gratings, to tailor the light absorption. Well-aligned dielectric or metallic gratings incorporated into Si NW PV devices were capable of tuning and amplifying the absorption efficiency upon controlling their pitches. The electrical metrics such as $V_{OC}$ were preserved after the integration of the grating. Therefore, our transfer method is not limited to the integration of the gratings only onto NWs but could be potentially exploited to fabricate more complex hybrid miniaturized structures for multifunctional nanoscale devices. We also believe that this study represents a meaningful step toward the development of three-dimensional optical and optoelectronic nanostructures.



DOI: 10.1021/acs.nanolett.7b03891
Nano Lett. 2017, 17, 7731−7736

## ■ ASSOCIATED CONTENT

### Supporting Information

The Supporting Information is available free of charge on the ACS Publications website at DOI: 10.1021/acs.nanolett.7b03891.

Detailed description of experimental methods and additional figures (PDF)

## ■ AUTHOR INFORMATION


### Corresponding Authors

*E-mail: sunkim@khu.ac.kr

*E-mail: hgpark@korea.ac.kr

### ORCID

James F. Cahoon: 0000-0003-1780-215X

Sun-Kyung Kim: 0000-0002-0715-0066

Hong-Gyu Park: 0000-0002-6375-0314


### Notes

The authors declare no competing financial interest.

## ■ ACKNOWLEDGMENTS

H.-G.P. acknowledges support from the National Research Foundation of Korea (NRF) grant funded by the Korean government (MSIT) (Nos. 2009-0081565, 2014M3A6B3063710 and 2017R1A4A1015426). S.-K.K. acknowledges support of this work by Basic Science Research Program through the NRF funded by the Ministry of Science, ICT, and Future Planning (NRF-2017R1A2B4005480). Y.-S.N. acknowledges support of this work by Basic Science Research Program through the NRF funded by the Ministry of Education (2017R1D1A1B03033668). J.F.C. and X.Z. acknowledge support by the Packard Fellowship for Science and Engineering and the National Science Foundation (DMR-1555001).

## ■ REFERENCES


(1) Kempa, T. J.; Day, R. W.; Kim, S.-K.; Park, H.-G.; Lieber, C. M. *Energy Environ. Sci.* **2013**, *6*, 719−733.

(2) Garnett, E. C.; Brongersma, M. L.; Cui, Y.; McGehee, M. D. *Annu. Rev. Mater. Res.* **2011**, *41*, 269−295.

(3) Lu, W.; Lieber, C. M. *Nat. Mater.* **2007**, *6*, 841−850.

(4) Cui, Y.; Lieber, C. M. *Science* **2001**, *291*, 851−853.

(5) Cui, Y.; Wei, Q.; Park, H.; Lieber, C. M. *Science* **2001**, *293*, 1289−1292.

(6) Tian, B.; Cohen-Karni, T.; Qing, Q.; Duan, X.; Xie, P.; Lieber, C. M. *Science* **2010**, *329*, 830−834.

(7) Cao, L.; Fan, P.; Vasudev, A. P.; White, J. S.; Yu, Z.; Cai, W.; Schuller, J. A.; Fan, S.; Brongersma, M. L. *Nano Lett.* **2010**, *10*, 439−445.

(8) Cao, L.; White, J. S.; Park, J.-S.; Schuller, J. A.; Clemens, B. M.; Brongersma, M. L. *Nat. Mater.* **2009**, *8*, 643−647.

(9) Krogstrup, P.; Jørgensen, H. I.; Heiss, M.; Demichel, O.; Holm, J. V.; Aagesen, M.; Nygard, J.; Fontcuberta i Morral, A. *Nat. Photonics* **2013**, *7*, 306−310.

(10) Kempa, T. J.; Cahoon, J. F.; Kim, S.-K.; Day, R. W.; Bell, D. C.; Park, H.-G.; Lieber, C. M. *Proc. Natl. Acad. Sci. U. S. A.* **2012**, *109*, 1407−1412.

(11) Kim, S.-K.; Song, K.-D.; Kempa, T. J.; Day, R. W.; Lieber, C. M.; Park, H.-G. *ACS Nano* **2014**, *8*, 3707−3714.

(12) Kim, S.-K.; Zhang, X.; Hill, D. J.; Song, K.-D.; Park, J.-S.; Park, H.-G.; Cahoon, J. F. *Nano Lett.* **2015**, *15*, 753−758.

(13) Kim, J.; Lee, H.-C.; Kim, K.-H.; Hwang, M.-S.; Park, J.-S.; Lee, J. M.; So, J.-P.; Choi, J.-H.; Kwon, S.-H.; Barrelet, C. J.; Park, H.-G. *Nat. Nanotechnol.* **2017**, *12*, 963−968.

(14) Cao, L.; Park, J.-S.; Fan, P.; Clemens, B.; Brongersma, M. L. *Nano Lett.* **2010**, *10*, 1229−1233.

(15) Hayden, O.; Agarwal, R.; Lieber, C. M. *Nat. Mater.* **2006**, *5*, 352−356.

(16) Yang, C.; Barrelet, C. J.; Capasso, F.; Lieber, C. M. *Nano Lett.* **2006**, *6*, 2929−2934.

(17) Wang, J.; Gudiksen, M. S.; Duan, X.; Cui, Y.; Lieber, C. M. *Science* **2001**, *293*, 1455−1457.

(18) Duan, X.; Huang, Y.; Agarwal, R.; Lieber, C. M. *Nature* **2003**, *421*, 241−245.

(19) Gradečak, S.; Qian, F.; Li, Y.; Park, H.-G.; Lieber, C. M. *Appl. Phys. Lett.* **2005**, *87*, 173111.

(20) Qian, F.; Li, Y.; Gradečak, S.; Park, H.-G.; Dong, Y.; Ding, Y.; Wang, Z. L.; Lieber, C. M. *Nat. Mater.* **2008**, *7*, 701−706.

(21) Duan, X.; Huang, Y.; Cui, Y.; Wang, J.; Lieber, C. M. *Nature* **2001**, *409*, 66−69.

(22) Gudiksen, M. S.; Lauhon, L. J.; Wang, J.; Smith, D. C.; Lieber, C. M. *Nature* **2002**, *415*, 617−620.

(23) Zhong, Z.; Qian, F.; Wang, D.; Lieber, C. M. *Nano Lett.* **2003**, *3*, 343−346.

(24) Qian, F.; Li, Y.; Gradečak, S.; Wang, D.; Barrelet, C. J.; Lieber, C. M. *Nano Lett.* **2004**, *4*, 1975−1979.

(25) Bao, J.; Zimmler, M. A.; Capasso, F.; Wang, X.; Ren, Z. F. *Nano Lett.* **2006**, *6*, 1719−1722.

(26) Tian, B.; Zheng, X.; Kempa, T. J.; Fang, Y.; Yu, N.; Yu, G.; Huang, J.; Lieber, C. M. *Nature* **2007**, *449*, 885−889.

(27) Kempa, T. J.; Tian, B.; Kim, D. R.; Hu, J.; Zheng, X.; Lieber, C. M. *Nano Lett.* **2008**, *8*, 3456−3460.

(28) Kim, S.-K.; Day, R. W.; Cahoon, J. F.; Kempa, T. J.; Song, K.-D.; Park, H.-G.; Lieber, C. M. *Nano Lett.* **2012**, *12*, 4971−4976.

(29) Day, R. W.; Mankin, M. N.; Gao, R.; No, Y.-S.; Kim, S.-K.; Bell, D. C.; Park, H.-G.; Lieber, C. M. *Nat. Nanotechnol.* **2015**, *10*, 345−352.

(30) Christesen, J. D.; Pinion, C. W.; Grumstrup, E. M.; Papanikolas, J. M.; Cahoon, J. F. *Nano Lett.* **2013**, *13*, 6281−6286.

(31) Lee, H.-C.; Na, J.-Y.; Moon, Y.-J.; Park, J.-S.; Ee, H.-S.; Park, H.-G.; Kim, S.-K. *Opt. Lett.* **2016**, *41*, 1578−1581.

(32) Ye, G.; Gong, Y.; Lin, J.; Li, B.; He, Y.; Pantelides, S. T.; Zhou, W.; Vajtai, R.; Ajayan, P. M. *Nano Lett.* **2016**, *16*, 1097−1103.

(33) Loewen, E. G.; Popov, E. *Diffraction Gratings and Applications*; Marcel Dekker: New York, 1997.

(34) Brundrett, D. L.; Gaylord, T. K.; Glytsis, E. N. *Appl. Opt.* **1998**, *37*, 2534−2541.

(35) Steele, J. M.; Moran, C. E.; Lee, A.; Aguirre, C. M.; Halas, N. J. *Phys. Rev. B: Condens. Matter Mater. Phys.* **2003**, *68*, 205103.




DOI: 10.1021/acs.nanolett.7b03891
*Nano Lett.* 2017, 17, 7731−7736